Liquid Crystals
Publication details, including instructions for authors and subscription information:
http://www.informaworld.com/smpp/title~content=t713926090

Converging flow of tumbling nematic liquid crystals

Alejandro D. Rey[ab]; Morton M. Denn[a]
[a] Department of Chemical Engineering, University of California at Berkeley, and Center for Advanced Materials, Lawrence Berkeley Laboratory, Berkeley, California, U.S.A. [b] Department of Chemical Engineering, McGill University, Montreal, Canada

To cite this Article Rey, Alejandro D. and Denn, Morton M.(1989) 'Converging flow of tumbling nematic liquid crystals', Liquid Crystals, 4: 3, 253 — 272
To link to this Article: DOI: 10.1080/02678298908029179
URL: http://dx.doi.org/10.1080/02678298908029179

LIQUID CRYSTALS, 1989, VOL. 4, NO. 3, 253–272

Converging flow of tumbling nematic liquid crystals

by ALEJANDRO D. REY† and MORTON M. DENN
Department of Chemical Engineering, University of California at Berkeley, and Center for Advanced Materials, Lawrence Berkeley Laboratory, Berkeley, California 94720, U.S.A.

(*Received 4 May, 1988; accepted 10 August 1988*)

A similarity solution of the Leslie–Ericksen equations is obtained for flow between converging planes for nematic liquid crystals which experience a tumbling instability ($\alpha_3 > 0$). The relative intensities of the stabilizing extensional flow near the centre plane, the destabilizing shear flow near the bounding plane, and the stabilizing Frank elasticity near both the boundary and the centre planes admit a variety of director distributions, depending on the rheological parameters; all distributions become unstable at critical values of the Ericksen number, leading to splay-bend walls for α_3 close to zero. A radial inhomogeneous magnetic field can suppress the instability. Closed-form analytical solutions are obtained for the transitions and the characteristic dimensions of splay-bend walls and boundary layers.

1. Introduction

The Leslie–Ericksen theory of the mechanics of nematic liquid crystals [1, 2, 3, 4] predicts that the liquids can become 'nonaligning' in shear flow if the viscosity coefficient α_3 becomes positive, leading to an inplane discontinuous transition in orientation known as *tumbling*. This phenomenon is also predicted by the liquid crystal theories of Hess [5, 6] and Helfrich [7]. Tumbling in shear flow has been observed experimentally [8, 9, 10, 11] and studied analytically and numerically [12, 13, 14, 15]. Agreement between the theoretical predictions and experiment has been demonstrated by Carlsson and Skarp [16] for steady flow between parallel plates and by Clark and coworkers [17] for oscillatory shear.

The question of flow alignment is of fundamental importance for the processing of nematic liquid crystalline polymers, where large orientation gradients are observed. The extent to which the Leslie–Ericksen (LE) theory approximates the behaviour of nematic polymers is unclear, since the full range of behaviour of this continuum theory has not been explored. The Leslie–Ericksen viscosities can be obtained from the low deformation rate limit of Doi's theory of liquid crystalline polymers [18]. (The Doi theory contains no analogue of the Oseen–Frank elasticity and cannot be applied to flows containing rapid changes in orientation.) α_3 as computed in the Doi theory is close to zero; whether it is computed to be slightly positive [19, 20] or slightly negative [21, 22] depends on the assumptions used in the analysis. Light scattering measurements of the Leslie–Ericksen viscosities in lyotropic liquid crystal polymers by Se and Berry [23] and Meyer and coworkers [24] would indicate negative α_3 and flow alignment.

† Present address: Department of Chemical Engineering, McGill University, Montreal, Quebec H3A 2A7, Canada.

0267–8292/89 $3.00

The introduction of elongational kinematics can cause new phenomena not found in simple shear flows [25, 26]. We extend our study of steady in-plane similarity solutions for two-dimensional converging flow (*Jeffrey–Hamel flow*) of nematic liquid crystals described by the LE continuum theory to flow regimes where periodic solutions and tumbling instabilities occur in simple shear. New phenomena are found because of the interaction of a stabilizing extensional component of the flow with the shear field. Solutions in which the director varies smoothly without large gradients (called *periodic solutions* by de Gennes [27]) are found for appropriate values of the rheological coefficients, while the introduction of elongation enables the existence of boundary layer behaviour as well. The boundary-layer regime gives rise to homogeneous structures with centreline regions containing rapidly-changing orientation distribution; these structures, for which multiple solutions of the nematic orientation with similar global free energies exist, are known as *splay-bend walls* and are analogous to Neel ferromagnetic walls [28]. The structure and appearance of the splay-bend walls can be altered by imposition of inhomogeneous magnetic fields. A schematic illustrating the qualitative difference between aligning ($\alpha_3 < 0$) and tumbling ($\alpha_3 > 0$) flow behaviour is shown in figure 1.

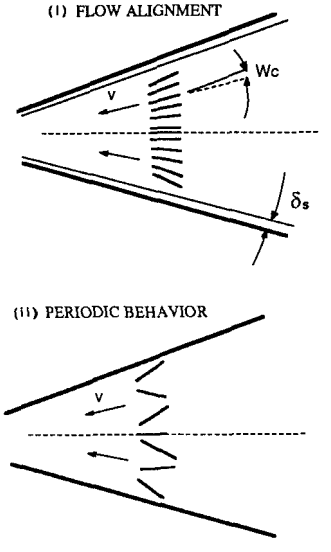

Figure 1. The two expected flow regimes for a nematic liquid crystal. (i) $\alpha_3 < 0$: characterized by bulk flow alignment in the radial direction and elastic boundary layers of thickness δ_s. (ii) $\alpha_3 > 0$: characterized by tumbling instabilities and periodic director orientation.

2. Balance equations and boundary conditions

The complete description of the mechanics of a nematic fluid requires the solution of the balance equations describing the velocity and orientation fields, which are coupled; the latter field is characterized by a unit vector **n**, known as the *director*. We have derived the balance equations for planar converging and diverging flow from the general Leslie–Ericksen theory in terms of similarity variables in [26]. Here we define the variables and present the equations.

Jeffrey–Hamel flows are described in a cylindrical (r, ψ, z) coordinate system; see figure 2. The radial distance r is measured from the vertex of the plates. The total

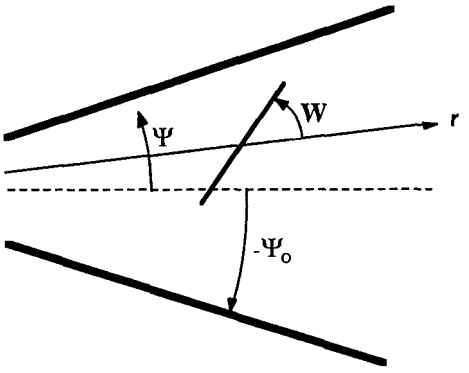

Figure 2. Schematic of Jeffrey–Hamel flow. $W(\psi)$ is the angle of the director with respect to a ray at angle ψ from the centerline. $\psi_0 = 0{\cdot}5$ in all calculations shown here.

enclosed angle between the plates is $2\psi_0$. We assume that the flow is radial, with no variation in the neutral (z) direction, so that $v_z = v_\psi = 0$. The non-zero radial component of velocity is then expressed in terms of the similarity variable $u(\psi)$ as follows:

$$v_r = \frac{u(\psi)}{r}. \tag{2.1}$$

$u(\psi)$ is negative for converging flow and positive for diverging flow. The isotropic pressure is of the following form:

$$p = \frac{\sigma(\psi)}{r^2} + \text{constant}. \tag{2.2}$$

We consider only flows in which the director is in the $\psi - r$ plane, in which case the two components are expressed in terms of the similarity variable $W(\psi)$ as follows:

$$n_r = \cos W(\psi), \quad n_\psi = \sin W(\psi), \tag{2.3}$$

The flow rate per unit width, q, is a fixed system constant:

$$q = \int_{-\psi_0}^{\psi_0} u(\psi)\, \mathrm{d}\psi. \tag{2.4}$$

The equations are non-dimensionalized by scaling the velocity with q and the elastic stresses with the coefficient of splay elasticity, K_{11}; the kinematics are then described by the following two dimensionless groups:

$$E = \frac{(\alpha_3 - \alpha_2)q}{K_{11}}, \tag{2.5a}$$

$$R = \frac{\varrho q}{\alpha_3 - \alpha_2}. \tag{2.5b}$$

E is the Ericksen number, which defines the relative weights of the viscous and elastic stresses. R is a pseudo-Reynolds number, which defines the relative weights of the inertial and viscous stresses. K_{11} is chosen as the normalizing elastic coefficient because the dominant deformation with planar boundary conditions is splay, and our simulation is far from the nematic–smectic transition at which K_{33} diverges [29, 30].

The linear momentum and director balance equations derived in [26] are then as follows:

$$g(1 + W')^2 + \varrho u^2 + a_1 u + a_2 uW' + a_3 u' + a_4 u'W' + a_5 u'' + 2\sigma = 0, \quad (2.6a)$$

$$\frac{g'}{2} - \frac{3}{2} g'(W')^2 - g'(W')^3 - 2gW'' - 2gW'W'' + a_6 u' + a_7 uW' + a_8 u'W' + a_9 u'' + a_{10} u - \sigma' = 0, \quad (2.6b)$$

$$\frac{g'}{2}(W'^2 - 1) + gW'' + [\lambda_2 \cos 2W + \lambda_1]\frac{u'}{2} + [\lambda_2 \sin 2W]u = 0, \quad (2.6c)$$

$$g(W) = K_{11}\cos^2 W + K_{33}\sin^2 W, \quad (2.7a)$$

$$g'(W) = (K_{33} - K_{11})\sin 2W, \quad (2.7b)$$

$$\lambda_1 = \alpha_2 - \alpha_3, \quad (2.8a)$$

$$\lambda_2 = \alpha_5 - \alpha_6. \quad (2.8b)$$

λ_1 and λ_2 are the rotational and irrotational viscosities, respectively. The coefficients $\{a_i\}$ $i = 1, \ldots 10$, which are tubulated in Appendix I, are functions only of the Leslie viscosities $\{\alpha_i\}$ and the function $W(\psi)$. For the special case $K_{11} = K_{33} = K$, which is used subsequently in some asymptotic analyses, $g(W) = K$ and $g'(W) = 0$.

Equations (2.6) are a set of coupled non-linear differential equations for the functions $W(\psi)$, $u(\psi)$, and $\sigma(\psi)$. The boundary conditions are as follows:

$$u'(0) = 0, \quad \text{symmetric velocity profile,} \quad (2.9a)$$

$$u(\pm\psi_0), = 0, \quad \text{no slip at the wall,} \quad (2.9b)$$

$$\sigma(\pm\psi_0) = \sigma_0, \quad \text{fixed reference pressure at the wall,} \quad (2.9c)$$

$$W(\pm\psi_0) = W_0, \quad \text{fixed anchoring angle at the wall,} \quad (2.9d)$$

$$W(0) = \begin{Bmatrix} \pm\pi/2 \\ 0 \end{Bmatrix}, \quad \text{centre line orientation.} \quad (2.9e)$$

Condition (2.9e) will be discussed in detail in §3.

All calculations were carried out using material parameters for the compound 4-*n*-octyl-4′-cyano biphenyl (8CB), as given by Kneppe and co-workers [31, 32] and Karat and Madhusudana [33]; the values are given in the table. It is convenient to

Physical constants for 8CB

Viscosities/Pa s	$e = -\alpha_3/\alpha_2$ 0·01	0·05	0·2	0·54	$e \geqslant 1$
α_1	0	0	0	0	0
α_2	−0·0585	−0·588	−0·0697	−0·0708	−0·07
α_4	0·06	0·06	0·06	0·06	0·06
α_5	0·0356	0·0394	0·0485	0·0627	0·07
α_6	−0·017	−0·0165	−0·007	0·0323	$-e\alpha_2$
Elastic constants (Newtons × 10^{11})					
K_{11}	1·0	1·03	1·28	1·41	1·45
K_{33}	0·9	0·95	1·37	2·09	2·39e

parametrize the behaviour through the ratio

$$e = -\alpha_3/\alpha_2 \tag{2.10}$$

here e is a strictly positive function of temperature for 8CB that changes sharply over a small (7°C) range. We have used assumptions of Carlsson and Skarp [16] that include $\alpha_1 = 0$, the Parodi [34] relation ($\alpha_6 - \alpha_5 = \alpha_2 + \alpha_3$) holds, and the critical behaviour of K_{33} is the same as that of α_3 as the smectic transition is approached. Solutions are restricted to values of e from zero to slightly greater than unity in order to avoid convergence problems associated with large values of e. This is not a serious restriction, since at temperatures for which $e > 1$ there is evidence that the hydrodynamic unit of 8CB ceases to behave as a rod because of strong dipole interactions [35, 36, 37].

Numerical solutions of the boundary value problem reported subsequently were obtained using the Galerkin finite element technique with linear shape functions over thirty spatial elements (e.g. Fletcher [38]). ψ_0 was taken as 0·5 in all cases. Newton–Raphson iteration was used for solution of the non-linear system of algebraic equations. Convergence was very sensitive in many cases to the selection of the initial estimates. Continuation was used to move through discontinuities at the limit points of the orientation profiles. Unstable solutions between branches were not calculated.

3. Centre-line orientation

Symmetry of the velocity profile and antisymmetry of the director orientation are assumed to exist around the center line, $\psi = 0$. There are multiple solutions to the equation set; these are characterized by aligned ($W = 0$) and transverse ($W = \pm\pi/2$) orientations at the centreline. Convergence to the correct solution can be ensured by using only the half-space $0 \leqslant \psi \leqslant \psi_0$ and setting the centerline boundary condition, rather than using symmetry. The boundary condition can be determined by a linear stability analysis, identical to the one carried out in [26], with the following result:

	$e < 1$	$e > 1$
In-flow	aligned	transverse
Out-flow	transverse	aligned

4. Similarity solutions

4.1. $e = 1$

An approximate analytical solution to equations (2.6) can be obtained for the case of $\alpha_2 = -\alpha_3$ ($e = 1$, $\lambda_2 = 0$) with the assumptions that $K_{11} = K_{33}$, $\alpha_1 = 0$, and that elastic stress contributions can be neglected in the linear momentum balance (equations (2.6 *a*, *b*)) but are retained in the torque balance (equation (2.6 *c*)). A decoupling of the linear momentum equation from the director equation is then suggested by evaluating the first two Miesowicz [39] viscosities (see, e.g., Chandrasekhar [40])

$$\eta_1 = \tfrac{1}{2}[\alpha_3 + \alpha_4 + \alpha_6], \tag{4.1 a}$$

$$\eta_2 = \tfrac{1}{2}[-\alpha_2 + \alpha_4 + \alpha_5]. \tag{4.1 b}$$

η_1 is the viscosity when the director is parallel to the flow, and η_2 is the viscosity when the director is parallel to the velocity gradient. If $\alpha_2 = -\alpha_3$ then $\eta_1 = \eta_2$ and the viscosity for in-plane flow becomes independent of orientation. The momentum

equation can thus be put into a form that is independent of director orientation and identical to that for a newtonian fluid, for which an analytical solution exists, e.g. [41]; in the limit $R = 0$ (and η_1 of the same order as α_3) this solution is

$$U(\psi) = \frac{u}{q} = \frac{\cos 2\psi - \cos 2\psi_0}{\sin 2\psi_0 - 2\psi_0 \cos 2\psi_0}. \tag{4.2}$$

The director equation (2.6*c*) with $\lambda_2 = 0$ is then

$$W'' + \frac{E}{2} U' = 0, \tag{4.3}$$

The solution for radial orientation at the centreline ($W(0) = 0$) is

$$W(\psi) = \frac{E}{2\gamma} [\psi \sin(1) - \tfrac{1}{2} \sin(2\psi)], \tag{4.4}$$

where

$$\gamma = \sin 2\psi_0 - 2\psi_0 \cos 2\psi_0. \tag{4.5}$$

The solution with transverse orientation ($W(0) = -\pi/2$) is

$$W = -\frac{E}{4\gamma} \sin 2\psi + \left[\frac{E}{2\gamma} \sin(1) + \pi\right] \psi - \frac{\pi}{2}. \tag{4.6}$$

To determine which profile is the more stable we use the principle of minimum entropy production (see, e.g., deGroot and Mazur [42], but note that Astarita [43] has demonstrated that that this principle is not universally applicable to non-newtonian fluids). The rate of entropy production per unit volume for the Leslie–Ericksen fluid is given by Leslie [1]; in terms of the similarity variables for this flow the equation is

$$T\dot{S} = (\alpha_2 + \alpha_3)\left(\frac{u'}{r^4}\right)\left[u \sin 2W - \frac{u'}{2} \cos 2W\right] + \frac{(\alpha_5 + \alpha_6)}{4}\left[\frac{u^2 + u'^2}{r^4}\right] + \left(\frac{\alpha_3 - \alpha_2}{4}\right)\left(\frac{u'^2}{r^4}\right) + \alpha_4\left[2\frac{u^2}{r^4} + \frac{1}{2}\frac{u'^2}{r^4}\right] \tag{4.7}$$

This simplifies for the special case $e = 1$ to

$$T\dot{S} = \left[\frac{-\alpha_2 + \alpha_4 + \alpha_6}{2}\right]\frac{u'^2}{r^4} + \left[\frac{\alpha_6}{2} + 2\alpha_4\right]\frac{u^2}{r^4} \tag{4.8}$$

and, as expected, the entropy production does not depend on the director orientation. Both profiles are thus equally stable by this criterion, and a transition from radial to transverse alignment at the centreline will occur if we impose a temperature program that causes the property ratio e to pass through unity. (This transition will undoubtedly have associated with it in practice a degree of super- or sub-cooling.) The calculated orientation profiles at $e = 1$ are shown in figure 3 for two values of the Ericksen number.

4.2. *General case: $e > 0$*

For the general case of positive e, equation (2.6) must be solved numerically. The centerline orientation is radial for $0 < e < 1$. Computed orientation profiles for $e = 0{\cdot}2$ are shown in figure 4 for a series of Ericksen numbers. The maximum angle

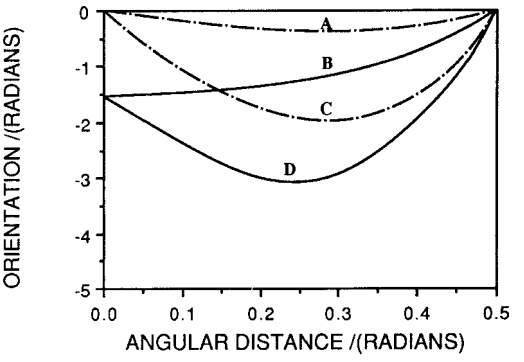

Figure 3. The two equally stable director distributions for the special case $e = 1$. A, B, $E = 12$; C, D, $E = 90$.

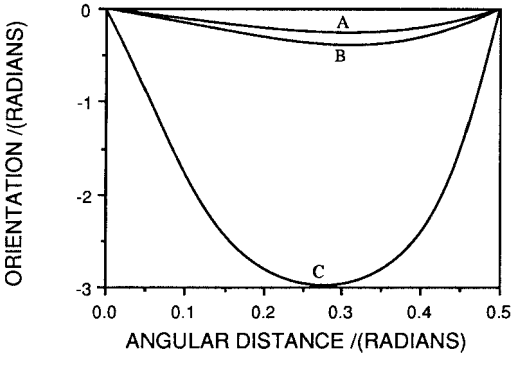

Figure 4. Director orientation profiles for $e = 0{\cdot}2$ before (A, B) and after tumbling (C). A, $E = 62{\cdot}4$; B, 84; C, 107. There is a discontinuous jump in the maximum angle between B and C.

increases smoothly with E until a critical value, after which it undergoes a discontinuous jump indicating the onset of tumbling. The maximum angle is shown in figure 5 as a function of the group $E/(1 + e)$ for three values of e. The series of discontinuous tumbling transitions for $e = 0{\cdot}2$, with multiple solutions and hysteresis characteristic of a 'fold catastrophe' [44], gives way to smooth behavior in a way that

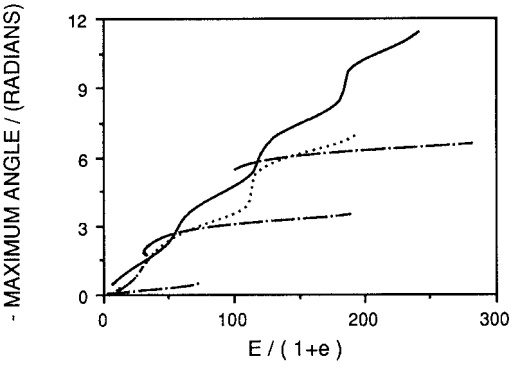

Figure 5. Magnitude of the maximum angle as a function of $E/(1 + e)$. –·–·–, $e = 0{\cdot}2$; ····, $e = 0{\cdot}54$; ——, $e = 1$.

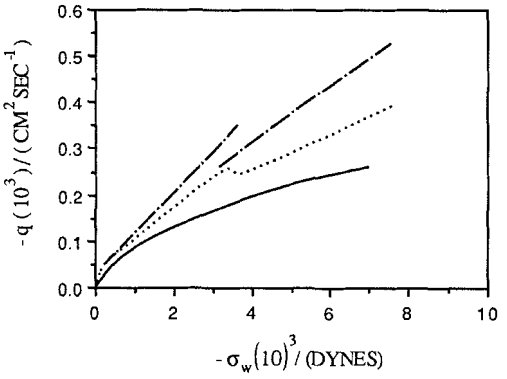

Figure 6. Magnitude of the flow rate per unit width (q) as a function of the reference wall pressure for various values of e; -·-·-, $e = 0{\cdot}2$; ····, $e = 0{\cdot}54$; ——, $e = 1$.

can be thought of as translating the instability to infinite values of E. As e increases towards unity the nematic behaves more and more like a newtonian fluid, as discussed previously. The results are replotted as flow rate per unit width versus the similarity variable for pressure (equivalent to a wall reference pressure at a fixed upstream position) in figure 6. Throughput initially increases with increasing upstream wall pressure for each value of e, as expected, but the effect of the tumbling transition is to cause a *decrease* in throughput as the pressure passes through a critical value; this is because the transverse orientation of a nematic liquid is more resistant to flow. (Carlsson [14] has analysed shear flow between parallel plates using the minimum entropy production principle, where the control variables are either the plate velocity or shear stress. These correspond to the flow rate, q, and the wall reference pressure, σ_0, respectively, in the present context.)

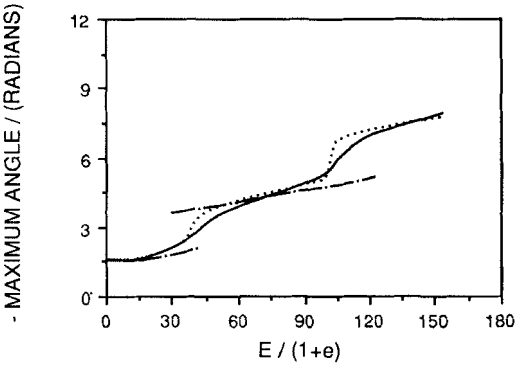

Figure 7. Magnitude of the maximum angle as a function of $E/(1 + e)$. ——, $e = 1$; ····, $e = 1{\cdot}2$; -·-·-, $e = 1{\cdot}5$.

Similar behaviour occurs for $e > 1$, but the centreline orientation is now transverse. The maximum angle is shown as a function of $E/(1 + e)$ in figure 7. The fluid behaves hydrodynamically as a newtonian liquid for $e = 1$, and the transitions in maximum angle sharpen with increasing e until the cascade of tumbling instabilities is again introduced.

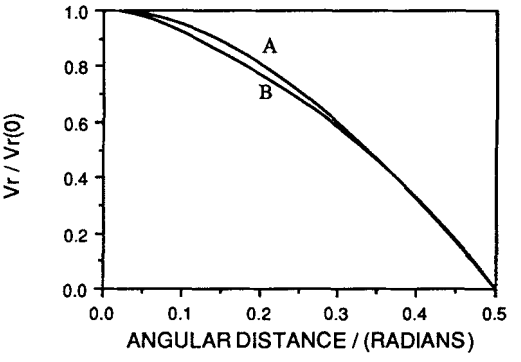

Figure 8. Scaled velocity profile just before the tumbling instability (A) and just after tumbling (B); $e = 0{\cdot}2$, $E = 36$.

The velocity profiles are relatively insensitive to the dramatic changes in the director profile at the onset of tumbling. The two velocity profiles shown in figure 8 for $e = 0{\cdot}2$ occur just before and after the director transition; the largest deviation in either profile from the one given by equation (4.2) is less than five percent.

5. Boundary layers and walls for $e \ll 1$

The presence of elongational torques in the neighbourhood of the centerplane in converging flow modifies the behaviour produced by a simple shear flow. One important example of this change is the possibility of boundary layer behaviour near the plate for $\alpha_3 > 0$, which is impossible for simple shear. (We use the terms 'plate' and 'boundary plane' for the solid surface in order to retain 'wall' for the splay-bend wall induced in the director orientation.) The stable angle of alignment of the director in the core (i.e., away from the bounding plane), W_c, where elastic stresses are not expected to be important, is readily shown in the absence of tumbling to be (c.f [26])

$$\tan W_c = (1 - e)\left(\frac{u}{u'}\right) + \sqrt{\left[(1 - e)^2\left(\frac{u}{u'}\right)^2 - e\right]}. \tag{5.1}$$

The argument of the radical becomes zero at a distance from the plate that depends on the magnitude of e; a good estimate for $e \ll 1$ is obtained by assuming a linear velocity profile close to the plate,

$$u = -\beta(\psi - \psi_0), \tag{5.2}$$

where β is a constant. The argument of the radical vanishes at a critical angle ψ^* given by

$$\psi^* = \psi_0 - \frac{\sqrt{e}}{1 - e}. \tag{5.3}$$

For $e \ll 1$ the core solution will extend very close to the plate, where it must undergo a rapid change to the induced boundary orientation. As e becomes larger the solution will change from the boundary-layer behaviour and will instead adopt a smooth (*periodic*) profile. Computed profiles illustrating the boundary layer behaviour for $e = 0{\cdot}01$ are shown in figure 9.

The orientation adopted by the director near the plate after the onset of tumbling retains the boundary layer structure, while the centreline region exhibits a splay-bend

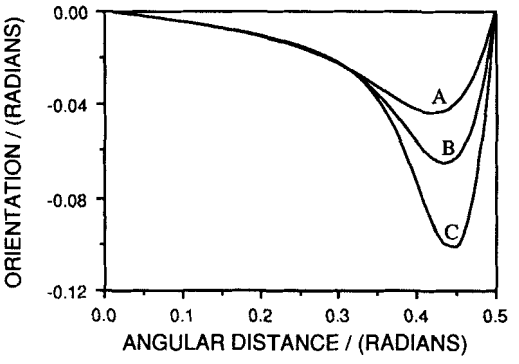

Figure 9. Orientation profile exhibiting boundary-layer behaviour for $e = 0{\cdot}01$, A, $E = 571$; B, 1146; C, 1757.

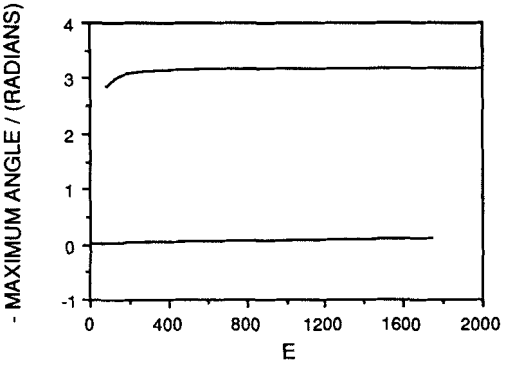

Figure 10. Maximum angle as a function of E for first tumbling, $e = 0{\cdot}01$.

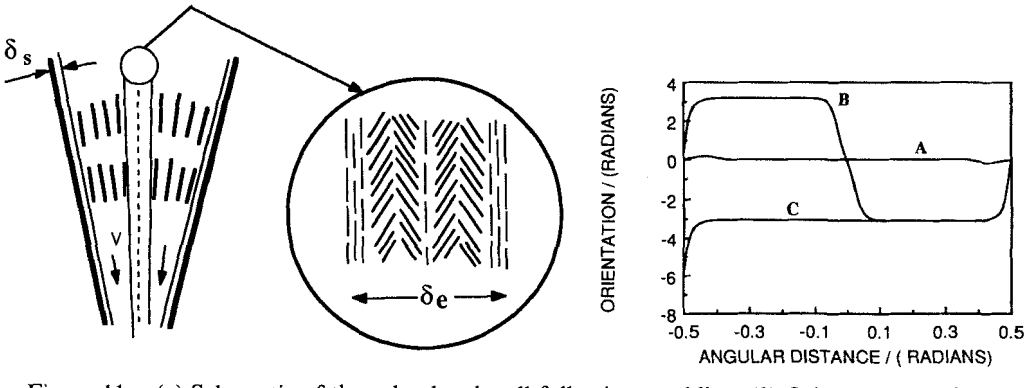

Figure 11. (*a*) Schematic of the splay-bend wall following tumbling. (*b*) Orientation profiles for aligned and tumbled solutions, $e = 0{\cdot}01$, $E = 1767$.

wall. The maximum angle remains close in magnitude to $n\pi$, $n = 0, 1, 2 \ldots$, where n is the number of tumbling instabilities; cf. figure 10 for the first tumbling. Two co-existing profiles at the first tumbling transition for $e = 0{\cdot}01$ are shown as curves A and B in figure 11 (*b*), where the splay-bend wall at the centreline following tumbling shown schematically in figure 11 (*a*) is clearly seen in curve B. The boundary layer at the plate in curve A, prior to tumbling, cannot be resolved on this scale. (Since walls

are narrow regions of high elastic energy, where the distortions of the director are large, the question naturally arises as to what other possible solutions are possible which might demand less elastic energy. Curve C in figure 11 is obtained by allowing the centreline orientation to be transverse at a value of $-\pi$, which is indistinguishable from the value of zero; solutions are possible for all stable centreline orientations of $W(0) = n\pi$, $n = 0, \pm 1, \pm 2, \ldots$. There does not appear to be any smooth way to obtain profile C with increasing Ericksen number without a large perturbation in the orientation.)

The critical Ericksen number at which tumbling occurs and the splay-bend wall arises at the centreline can be estimated for $e \ll 1$ using a singular perturbation analysis to obtain the bounding plane (inner) solution that matches the core (outer) solution given by equation (5.1). The detailed treatment is contained in Appendix II. One arbitrary constant of order unity, corresponding to the fractional value of $\psi^* - \psi_0$ at which smooth inner and outer solutions are matched, must be introduced; the value used for the best results is 6/5. The critical Ericksen number at which the first tumbling transition occurs is found to be

$$E_c = -\frac{10[\sqrt{e} - a(\psi^* - \psi_0)]}{7U'_w e(\psi^* - \psi_0)}. \tag{5.4}$$

Here $U'_w = U'(\psi_0)$. ψ^* is given by equation (5.3) and a by

$$a = \frac{(1 - e)\sqrt{e}}{(1 + e)\sqrt{e} + \frac{6}{5}(1 - e^2)(\psi^* - \psi_0)}. \tag{5.5}$$

An estimate of the boundary layer thickness is given by

$$\delta_s = \frac{C}{-U'_w e\sqrt{E}}, \tag{5.6}$$

with

$$C = -\frac{a}{\sqrt{E_c}}\left[1 + \frac{6}{5}\frac{U'_w e(\psi^* - \psi_0)}{a}\right]. \tag{5.7}$$

The critical Ericksen number for the onset of tumbling predicted by equation (5.4) is plotted as a function of e for $e \ll 1$ in figure 12, together with values obtained from the complete numerical solution. Agreement is extremely good.

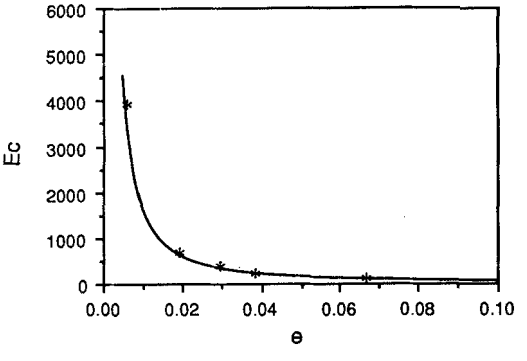

Figure 12. Comparison of singular perturbation analysis with numerical solutions for the critical values of the Ericksen number, E_c, as a function e.

6. Magnetohydrodynamics

The balance equations for inhomogeneous radial and azimuthal magnetic fields in converging and diverging flows of LE fluids were derived in [26], where the motivation was to study the possibility of controlling orientation distribution. We explore here the possibility of changing the onset of tumbling by applying radial magnetic fields. A similar problem using an electric field in shear flow as analysed by Carlsson and Skarp [45].

Compatibility with the similarity transformation and the Maxwell equations requires that the magnetic field have the following form:

$$H = \left[\frac{A}{r}, \frac{B}{r}, 0\right]. \tag{6.1}$$

The dimensionless group that appears in the balance equations (see [26]) is the Zocher number, Z

$$Z^2 = \frac{(A^2 + B^2)\Delta\chi}{K_{11}}. \tag{6.2}$$

$\Delta\chi$ is the anisotropic magnetic susceptibility. The Zocher number gives the relative magnitude of magnetic to elastic torques; the relative magnitude of viscous to magnetic torques is given by

$$D = \frac{E}{Z^2} = \frac{-\alpha_2(1 + e)q}{(A^2 + B^2)\Delta\chi}. \tag{6.3}$$

The anisotropic magnetic susceptibility of 8CB is of the order of 10^{-6}, which is typical for liquid crystals [46] (the SI value for magnetic susceptibility is obtained by multiplying the unrationalized cgs value by 4π; the cited literature data use the latter); temperature-dependent values are given in [47], but all calculations were carried out in terms of dimensionless variables.

A radial magnetic field influences the flow in two ways: the field induced director alignment in the radial direction, thus stabilizing the shear-induced instability; the field also causes a position-dependent body force. The latter causes an effective pressure gradient that acts against the flow and hence retards the motion and reduces the Ericksen number for a fixed wall reference pressure. The effect of an azimuthal field on converging flow is qualitatively different. The magnetic body force still acts to retard the flow, but the field tends to induce a transverse alignment during inflow and therefore destabilize the alignment of the director even further.

The stabilizing effect of a radial field is readily demonstrated by an analysis analogous to that in §5. The outer (core) solution for the director orientation in the absence of elastic effects is given by

$$\tan W_c = \left[(1 - e)\left(\frac{U}{U'}\right) + \frac{1 + e}{2DU'}\right] + \sqrt{\left\{\left[(1 - e)\left(\frac{U}{U'}\right) + \frac{1 + e}{2DU'}\right]^2 - e\right\}} \tag{6.4}$$

where the positive sign is chosen for stability reasons. The maximum angle possible without tumbling then follows from the vanishing of the argument of the radical to be

$$\tan W_{c,\max} = -\sqrt{e} \tag{6.5}$$

and the critical value of $D(=D_c)$ beyond which tumbling cannot occur is

$$D_c = -\frac{1+e}{2U'_w\sqrt{e}}. \tag{6.6}$$

A singular perturbation analysis analogous to the one in Appendix II results in a first approximation to the inner solution that is not amenable to further analysis, so a full numerical solution is required to proceed further for values of $D < D_c$. The surface of critical Ericksen numbers for the tumbling transition is shown in figure 13 in terms of D and e. As expected, a given field intensity will have the greatest stabilizing effect for small e, for the reason that the shear torques are less destabilizing then. As e is increased (i.e. the temperature is lowered) strong radial fields will be necessary to suppress the tumbling for a given flow rate. The intersection of the surface with the $(1/D, e)$ plane as $E_c \to \infty$ defines D_c as given by equation (6.6).

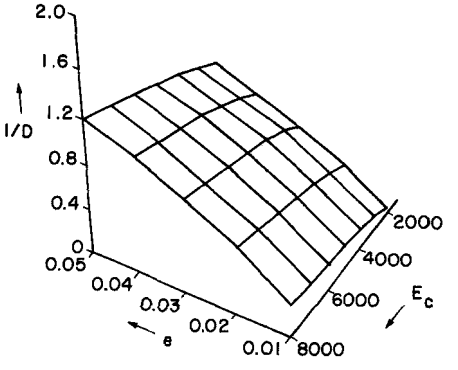

Figure 13. Three-dimensional stability space of 8CB in Jeffrey–Hamel flow.

7. Splay-bend walls

We analyse here the wall-like structures that can be created by flow alone, and by the interaction of flow and non-homogeneous magnetic fields. The walls which we are treating here are similar to those first discussed by Helfrich [28] for static deformations; they are of the splay-bend type, because splay and bend are the curvature strains present.

To address the splay-bend walls that result from the tumbling instability in the plate boundary-layer regime ($e \ll 1$) we again pursue a singular perturbation analysis, but we now also look for a boundary layer at the centreline. Details are contained in Appendix II. The thickness $\delta_c(E)$ of the splay-bend wall about the centreline ($\psi = 0$) is then found to be

$$\delta_c(E) = \frac{2}{\sqrt{[2(1-e)U_0E]}}. \tag{7.1}$$

Here, $U_0 = U(0)$. The corresponding boundary layer thickness at the bounding plane $\psi = \psi_0$ is

$$\delta_s(E) = \sqrt{\left(\frac{2\pi}{-U'_w eE}\right)}. \tag{7.2}$$

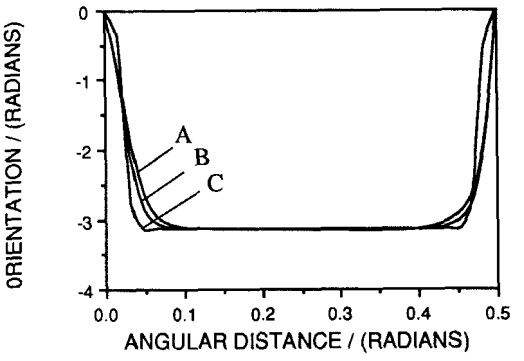

Figure 14. Effect of a radial magnetic field on wall thickness. $e = 0{\cdot}01$, $E = 1767$; *A*, $Z^2 = 0$; *B*, 2360; *C*, 31508.

For the general case of m-tumbling instabilities we just modify the numerator in equation (7.2) by replacing 2π with $2m\pi$. In this case the director undergoes a rotation of $2m\pi$ radians in traversing the wall, which is parallel to the flow direction.

When an inhomogeneous radial magnetic field, $H = (A/r, 0, 0)$, is applied to the tumbled flow we expect to obtain narrowing of the splay-bend centreline wall, and this is observed; cf. figure 14. The qualitative features are otherwise unchanged from the tumbled flow in the absence of a field. The singular perturbation estimate of the centreline wall thickness is modified by inclusion of the Zocher number to

$$\delta_c(E, Z) = \frac{2}{\sqrt{[2(1 - e)U_0E + Z^2]}}. \tag{7.3}$$

In contrast, the application of a sufficiently strong transverse magnetic field, $\mathbf{H} = (0, B/r, 0)$, to the tumbled flow will result in a splay-bend wall perpendicular to the field; the director rotates only π radians in traversing the wall. Orientation profiles for different azimuthal field strengths are shown in figure 15. The wall thickness is increased, with the singular perturbation estimate of

$$\delta_c(E, Z) = \frac{2}{\sqrt{[-2(1 - e)U_0E + Z^2]}}. \tag{7.4}$$

(Equation (7.4) is valid only for $Z^2 \gg 4/\psi_0^2 + 2(1 - e)U_0E$.)

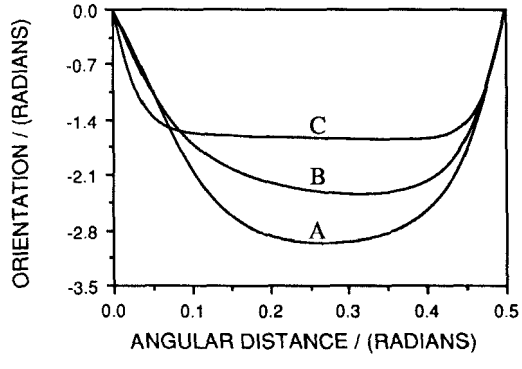

Figure 15. Effect of an azimuthal magnetic field on tumbled solutions. $e = 0{\cdot}01$; *A*, $E = 160$, $Z^2 = 81$; *B*, 150, 492; *C*, 58, 1896.

Since the solution of the equations of motion has been restricted to director orientations that are two-dimensional, the possible 'escape' of the director into the third dimension has not been taken into account. We have found magnetically-induced walls to be unstable in some cases for non-tumbling nematics [48] with large differences between splay and twist elasticity coefficients, and these structures might also be hydrodynamically unstable under some conditions to perturbations out of the plane. This question seems especially relevant in the case of polymeric nematics, where it has been proposed that high energy splay deformations are avoided by a twist out of the plane (see Meyer [49]).

8. Concluding remarks

The characteristics of converging flow of tumbling nematics in the absence of an external field are summarized in figure 16, which is a schematic of configurations and transitions on the Ericksen number-e plane; increasing e corresponds to a decreasing temperature. For small but positive e the director profile exhibits boundary-layer behaviour, with a tumbling transition at a critical value of E to a configuration with a surface boundary layer and a splay-bend wall at the midplane. With increasing e the boundary layer transforms to a periodic distribution, with a maximum angle that increases with flow rate. There is a critical value of E in this regime at which the tumbling transition occurs, but to a periodic tumbled state with a radial centreline orientation.

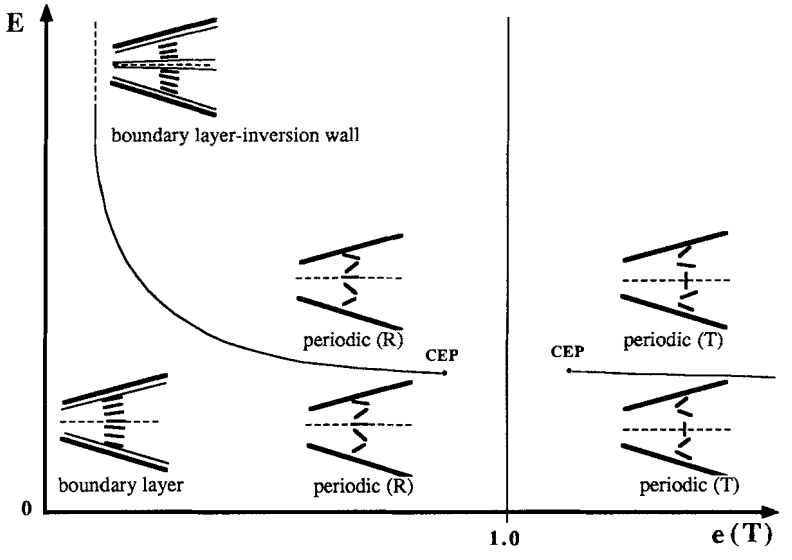

Figure 16. Schematic of flow configurations and phase transitions in the $E - e$ plane for tumbling nematics.

There is a window of stability in the neighbourhood of $e = 1$. Radial and transverse centreline profiles are energetically equal at $e = 1$, with an exchange of stability between the two configurations as $e = 1$ is traversed. Further increase in e reintroduces the tumbling transition, with periodic profiles having a transverse centreline orientation. (Such a stability window, in which tumbling disappears at the

temperature at which $e = 1$, has been recorded in shearing experiments by Cladis and Torza [9].)

Carlsson [14] has noted that it is instructive to regard tumbling as analogous to a first-order non-equilibrium phase transition. If we adopt this viewpoint, then we find that in addition to the coexistence line of first-order transitions in converging flow there are two critical end points (CEP) limiting the stability window. Furthermore, for $e \ll 1$ the transition occurs with the simultaneous appearance of wall defects, and is thus a new instance of the analogous equilibrium defect-mediated phase transition [50].

This work was supported in part by the Donors of the Petroleum Research Fund (ADR) and in part by the Director, Office of Energy Research, Office of Basic Energy Sciences, Materials Science Division of the U.S. Department of Energy under Contract No. DE-AC03-76SF00098 (MMD), supplemented by a gift from E. I. DuPoint de Nemours & Co., Inc.

Appendix I

The coefficients (a_i) in equations (2.7) are as follows:

$$a_1 = \alpha_1 \cos 2W + (\alpha_5 + \alpha_6)\cos 2W, \tag{I 1a}$$

$$a_2 = -\alpha_1 \cos 4W - (\alpha_5 - \alpha_6)\cos 2W, \tag{I 1b}$$

$$a_3 = -\alpha_1 \cos W^2 \sin 2W - \alpha_5 \sin 2W, \tag{I 1c}$$

$$a_4 = \frac{\alpha_1}{2}\sin 4W + (\alpha_5 - \alpha_6)\sin 2W, \tag{I 1d}$$

$$a_5 = \frac{\alpha_1}{2}\sin^2 2W + \left(\frac{\alpha_5 - \alpha_2}{2}\right)\sin^2 W + \left(\frac{\alpha_3 + \alpha_6}{2}\right)\cos^2 W + \frac{\alpha_4}{2}, \tag{I 1e}$$

$$a_6 = -\alpha_1 \sin^2 W \cos 2W + \alpha_4 + 2\alpha_5 \sin^2 W + \alpha_3, \tag{I 1f}$$

$$a_7 = \alpha_1(1 - 2\cos 2W)\sin 2W + (\alpha_5 + \alpha_6)\sin 2W, \tag{I 1g}$$

$$a_8 = \frac{\alpha_1}{2}(\cos 2W - \cos 4W) + \alpha_6 \cos 2W, \tag{I 1h}$$

$$a_9 = \alpha_1 \sin^3 W \cos W + \alpha_6 \sin W \cos W, \tag{I 1i}$$

$$a_{10} = (\alpha_6 - \alpha_5)\sin 2W. \tag{I 1j}$$

The Parodi relation, $\alpha_6 - \alpha_5 = \alpha_2 + \alpha_3$, has been used to simplify some equations.

Appendix II

Singular perturbation analysis for $e \ll 1$

The director equation (2.6c) in non-dimensional form is

$$\frac{1}{E}W'' + \left[\frac{-(1-e)}{(1+e)}\cos 2W + 1\right]\frac{U'}{2} - \left[\frac{(1-e)}{(1+e)}\sin 2W\right]U = 0, \tag{II 1}$$

where U is given by equation (4.2). To focus on the elastic boundary layer we define a stretching transformation, as follows:

$$W(\psi) = W_i(\eta), \tag{II 2a}$$

$$\psi - \psi_0 = \xi(E)\eta. \tag{II 2b}$$

To balance second order terms in equation (II 1) we require that $\xi(E) = 1/\sqrt{E}$, in which case equation (II 2*b*) becomes

$$\psi - \psi_0 = \eta/\sqrt{E}. \tag{II 3}$$

In the transformed variables equation (II 1) then becomes

$$W_i'' + \left[\frac{-(1-e)}{(1+e)}\cos 2W_i + 1\right]\frac{U'(\psi)}{2} - \left[\frac{(1-e)}{(1+e)}\sin 2W_i\right]U(\psi) = 0. \tag{II 4}$$

$U(\psi)$ is now expanded in a power series about $\psi = \psi_0$, using the fact that $U(\psi_0) = 0$, leading to the following form for the boundary layer equation:

$$W_i'' + \left[\frac{-(1-e)}{(1+e)}\cos 2W_i + 1\right]\frac{U_w'}{2} = 0. \tag{II 5}$$

Here $U_w = U(\psi_0)$. For the case of present interest $e \ll 1$ and $W_i \ll 1$, in which case we finally obtain

$$W_i'' + eU_w = 0. \tag{II 6}$$

Equation (II 6) is integrated twice, using the condition $W_i(\psi_0) = 0$, to obtain the first inner expansion in terms of the outer variable ψ as

$$W_i(\psi) = -\frac{U_w'}{2}Ee(\psi - \psi_0)^2 + C_2\sqrt{E}(\psi - \psi_0). \tag{II 7}$$

To evaluate the constant C_2 we have to match equations (II 7) and the outer (core) solution given by (5.1). Because the outer equation defining W_c is algebraic the usual limiting procedures for inner–outer expansions cannot be employed. We choose to match the derivatives at a position that is of order ψ^*; matching at $\psi - \psi_0 = 1.2(\psi^* - \psi_0)$ gives good agreement with computed values, leading to the following equation:

$$W_i(\psi) = \frac{-U_w'}{2}Ee(\psi - \psi_0)^2 + 1{\cdot}2U_w'\sqrt{(E_cE)}e(\psi - \psi_0)(\psi^* - \psi_0) + a\sqrt{(E/E_c)}(\psi - \psi_0), \tag{II 8}$$

where a is given by equation (5.5).

To find the critical Ericksen number at which tumbling occurs for $e \ll 1$ we match the inner and outer solutions at the critical point ψ^*, which leads to the following result:

$$E_c = -\frac{10[\sqrt{[e - a(\psi^* - \psi_0)]}]}{7U_w'e(\psi^* - \psi_0)}. \tag{II 9}$$

The estimate of the boundary layer thickness δ_s in equation (5.6) is obtained by setting the derivative of W_i to zero and defining that point as δ_s.

An analogous perturbation analysis is carried out to analyse the splay-bend walls about the centerplane for $e \ll 1$. The stretched variable near the centerline is

$$\psi = \eta/\sqrt{E}. \tag{II 10}$$

Equation (II 4) is unchanged, but for the expansion about $\eta = 0$ we now use the fact that $U_0' = U'(0) = 0$. The first inner expansion is then a solution of

$$W_i'' - \left[\frac{(1-e)}{(1+e)}\sin 2W_i\right]U_0 = 0, \tag{II 11}$$

where $U_0 = U(0)$. It is convenient to define a translated dependent variable by

$$y = W_i + \pi. \tag{II 12}$$

Expanding equation (II 11) for $e \ll 1$ and small y (i.e. W_i close to $-\pi$ radians) we then obtain

$$y'' - 2(1 - e)U_0 y = 0. \tag{II 13}$$

The first inner expansion in terms of the outer variable is

$$y(\psi) = C \exp\{-\sqrt{[2(1 - e)U_0 E]}\psi\}. \tag{II 14}$$

We would obtain an approximation that satisfies the centreline condition by taking $C = \pi$, but that would violate the assumption that y is small and a value of C is not needed in order to compute the wall thickness. The boundary layer thickness $\delta_e(E)$ is estimated by doubling the value of ψ for which the argument of the exponential becomes -1,

$$\delta_e(E) = \frac{2}{\sqrt{[2(1 - e)U_0 E]}}. \tag{II 15}$$

The boundary layer thickness near $\psi = \psi_0$ following tumbling is obtained by using the stretched coordinate given by equation (II 3) which, for small e and W_i close to $-\pi$, leads to the equation

$$y'' + eU_w' = 0. \tag{II 16}$$

The solution with $y(0) = \pi$ and $y'(-\delta\sqrt{E}) = 0$ is

$$y = -\frac{eU_w'}{2}\eta^2 + eU_0'\delta\eta + \pi. \tag{II 17}$$

We can then estimate the boundary layer thickness $\delta_s(E)$ by assuming that $y(\delta_s) = 0$, giving

$$\delta_s(E) = \sqrt{\left(\frac{2\pi}{-U_w' eE}\right)}. \tag{II 18}$$

For the general case of m-tumbling instabilities we replace the 2π in the numerator by $2m\pi$.

The analysis is essentially unchanged by inclusion of a radial magnetic field of the form $H = (A/r, 0, 0)$. The splay-bend wall is again parallel to the flow direction and to the radial field. The boundary layer thickness is modified by the presence of the field, and the singular perturbation analysis now gives a first inner approximation valid around $y \sim 0$ of

$$y(\psi) = C \exp\{-\sqrt{[2(1 - e)U_0 E + Z^2]}\psi\} \tag{II 19}$$

and a wall thickness of order

$$\delta_e(E, Z) = \frac{2}{\sqrt{[2(-e)U_0 E + Z^2]}}. \tag{II 20}$$

Application of a transverse field of the form $H = (0, B/r, 0)$ to the tumbled director field will result in a splay-bend wall perpendicular to the field for a sufficiently strong field. The director will now rotate a total of π radians by transversing the wall.

The presence of an azimuthal field changes the director equation to

$$\frac{1}{E}W'' + \left[\frac{-(1-e)}{(1+e)}\cos 2W + 1\right]\frac{U'}{2} - \left[\frac{(1-e)}{(1+e)}\sin 2W\right]U + \frac{1}{2D}\sin 2W = 0. \tag{II 21}$$

The core (outer) solution is readily obtained by letting $1/E \to 0$,

$$\tan W_c = \left[(1-e)\left(\frac{U}{U'}\right) - \frac{1+e}{2DU'}\right] + \sqrt{\left\{\left[(1-e)\left(\frac{U}{U'}\right) - \frac{1+e}{2DU'}\right]^2 - e\right\}}. \tag{II 22}$$

The inner solution is obtained by translating the director angle by $\pi/2$ to

$$y = W + \pi/2 \tag{II 23}$$

and defining the stretched variable about the centreplane by equation (II 10), in which case the first inner expansion is a solution of

$$y'' - \left[\frac{(1-e)}{(1+e)}\sin 2y\right]U_0 - \frac{1}{2D}\sin 2y = 0. \tag{II 24}$$

For small y and $e \ll 1$ this becomes

$$y'' - \left[2(1-e)U_0 - \frac{1}{D}\right]y = 0, \tag{II 25}$$

with a solution

$$y(\psi) = C\exp\{-\sqrt{[-2(1-e)U_0E + Z^2]}\psi\}. \tag{II 26}$$

The thickness of the splay-bend wall is then

$$\delta_e(E, Z) = \frac{2}{\sqrt{[-2(1-e)U_0E + Z^2]}}. \tag{II 27}$$

This solution requires that the field be sufficiently strong to create a wall of thickness greater than ψ_0, or $Z^2 \gg 4/\psi_0^2 + 2(1-e)U_0E$.

References

[1] LESLIE, F. M., 1966, *Q. J. Mech. appl. Math.*, **19**, 357.
[2] LESLIE, F. M., 1968, *Archs Ration. mech. Anal.*, **28**, 265.
[3] ERICKSEN, J. L., 1960, *Archs Ration. mech. Anal.*, **4**, 231.
[4] DE GENNES, P. G., 1975, *The Physics of Liquid Crystals*, (Oxford University Press).
[5] HESS, S., 1975, *Z. Naturf.* A, **30**, 1224.
[6] HESS, S., 1976, *Z. Naturf.* A, **31**, 1034.
[7] HELFRICH, W., 1970, *J. chem. Phys.*, **53**, 2267.
[8] CLADIS, P. E., and TORZA, S., 1975, *Phys. Rev. Lett.*, **35**, 1283.
[9] CLADIS, P. E., and TORZA, S., 1976, *Colloid and Interface Science*, Vol. IV (Academic Press), p. 487.
[10] PIERANSKI, P., and GUYON, E., 1975, *Phys. Rev. Lett.*, **32**, 924.
[11] PIERANSKI, P., GUYON, E., and PIKIN, S., 1976, *J. Phys. Paris, Colloq.*, **37**, Cl, 3.
[12] PIKIN, S. A., 1974, *Sov. Phys. JETP*, **38**, 1246.
[13] MANNEVILLE, P., 1981, *Molec. Crystals liq. Crystals*, **70**, 223.
[14] CARLSSON, T., 1984, *Molec. Crystals liq. Crystals*, **104**, 307.
[15] HÖGFORS, C. and CARLSSON, T., 1984, manuscript contained in T. Carlsson, Ph.D. Dissertation, Chalmers University of Technology, Göteborg.

[16] CARLSSON, T., and SKARP, K., 1986, *Liq. Crystals*, **1**, 455.
[17] CLARK, M. G., SAUNDERS, F. G., SHANKS, I. A., and LESLIE, F. M., 1986, *Molec. Crystals liq. Crystals*, **70**, 195.
[18] DOI, M., and EDWARDS, S. F., 1986, *The Theory of Polymer Dynamics* (Clarendon Press).
[19] KUZUU, N., and DOI, M., 1983, *J. phys. Soc. Japan*, **52**, 3486; 1984, *Ibid.*, **53**, 1031.
[20] SEMENOV, A. N., 1983, *Sov. Phys. JETP*, **58**, 321.
[21] MARRUCI, G., 1982, *Molec. Crystals liq. Crystals*, **72L**, 153.
[22] DOI, M., 1983, *Faraday Symp. Chem. Soc.*, **18**, 49.
[23] SE, K., and BERRY, G. C. 1987, *Molec. Crystals liq. Crystals*, **153**, 133.
[24] TARATUTA, V., HURD, A. J., and MEYER, R. B., 1985, *Phys. Rev. Lett.*, **55**, 246.
[25] REY, A. D., and DENN, M. M., 1987, *Molec. Crystals liq. Crystals*, **153**, 301.
[26] REY, A. D., and DENN, M. M., 1988, *J. Non-Newton. Fluid Mech.*, **27**, 375; see also Corrigenda (in the press).
[27] DE GENNES, P. G., 1972, *Physics Lett.* A, **4**, 479.
[28] HELFRICH, W., 1968, *Phys. Rev. Lett.*, **21**, 1518.
[29] DE GENNES, P. G., 1972, *Solid St. Commun.*, **10**, 753.
[30] CHEUNG, L., MEYER, R. B., and GRUBER, H., 1973, *Phys. Rev. Lett.*, **31**, 343.
[31] KNEPPE, H., SCHNEIDER, F., and SHARMA, N. K., 1981, *Ber Bunsenges. phys. Chem.*, **85**, 784.
[32] KNEPPE, H., SCHNEIDER, F., and SHARMA, N. K., 1982, *J. chem. Phys.*, **77**, 3203.
[33] KARAT, P. P., and MADHUSUDANA, N. V., 1977, *Molec. Crystals liq. Crystals*, **40**, 239.
[34] PARODI, O., 1970, *J. Phys.*, **31**, 581.
[35] DE JEU, W. H., 1983, *Phil. Trans. Soc.* A, **303**, 217.
[36] LEADBETTER, A. J., RICHARDSON, R. M., and COLLING, C. N., 1975, *J. Phys., Paris*, **36**, C1-37.
[37] LYDON, J. E., and COAKLEY, C. J., 1975, *J. Phys., Paris*, **36**, C1-45.
[38] FLETCHER, C. A. J., 1984, *Computational Galerkin Methods* (Springer-Verlag).
[39] MIESOWICZ, M., 1946, *Nature, Lond.*, **158**, 27.
[40] CHANDRASEKHAR, S., 1977, *Liquid Crystals* (Cambridge University Press).
[41] DENN, M. M., 1980, *Process Fluid Mechanics* (Prentice-Hall, Inc.).
[42] DE GROOT, S. R., and MAZUR, P., 1962, *Non-Equilibrium Thermodynamics* (North-Holland Publishing Company).
[43] ASTARITA, G., 1977, *Non-Newton. Fluid Mech.*, **2**, 343.
[44] THOM, R., 1975, *Structural Stability and Morphogenesis* (Benjamin).
[45] CARLSSON, T., and SKARP, R., 1981, *Molec. Crystals liq. Crystals*, **78**, 157
[46] MOORE, R. C., and DENN, M. M., 1988, *High Modulus Polymers: Approaches to Design and Development*, edited by A. E. Zachariades and R. S. Porter (Marcel Dekker).
[47] BRADSHAW, M. J., RAYNES, E. P., BUNNING, J. D., and FABER, T. E., 1985, *J. Phys., Paris*, **46**, 1513.
[48] REY, A. D., 1988, Ph.D. Dissertation (University of California at Berkeley).
[49] MEYER, R. B., 1982, *Polymer Liquid Crystals*, edited by A. Ciferri, W. R. Krigbaum and R. B. Meyer (Academic Press).
[50] NELSON, D. R., 1980, *Fundamental Problems in Statistical Mechanics*, edited by E. G. D. Cohen (North Holland).